Aqueous Formulation of Concentrated Semiconductive Fluid Using Polyelectrolyte Coacervation

My Linh Le,† Dakota Rawlings,‡ Scott P. O. Danielsen,§ Rhys M. Kennard,† Michael L. Chabinyc,† and Rachel A. Segalman.† ‡

† Materials Department, University of California, Santa Barbara, CA, 93106

‡ Chemical Engineering Department, University of California, Santa Barbara, CA, 93106

§ Thomas Lord Department of Mechanical Engineering and Materials Science, Duke University, Durham, NC, 27708

To whom correspondence should be addressed: segalman@ucsb.edu and *mchabinyc@engineering.ucsb.edu*

Abstract

Conjugated polyelectrolytes (CPEs), which combine π-conjugated backbones with ionic side chains, are intrinsically soluble in polar solvents and have demonstrated tunability with respect to solution processability and optoelectronic performance. However, this class of polymer often suffers from limited solubility in water. Here, we demonstrate how polyelectrolyte coacervation can be utilized for aqueous processing of conjugated polymers at extremely high polymer loading. Sampling various mixing conditions, we identify compositions that enable the formation of complex coacervates of an alkoxysulfonate-substituted PEDOT (PEDOT-S) with poly(3-methyl-1-propylimidazolylacrylamide) (PA-MPI). The resulting coacervate is a viscous fluid containing 50% *w/v* polymer and can be readily blade-coated into films of (4 ± 0.5) μm thick. Subsequent acid doping of the film increased the electrical conductivity of the coacervate to twice that of the doped neat PEDOT-S film. This higher conductivity of the doped coacervate film suggests an enhancement in charge carrier transport along PEDOT-S backbone, in agreement with spectroscopic data which shows an enhancement in the conjugation length of PEDOT-S upon coacervation. This study illustrates the utilization of electrostatic interactions in aqueous processing of conjugated polymers, which will be useful in large-scale industrial processing of semiconductive materials using limited solvent, and with added enhancements to the optoelectronic properties of the material.

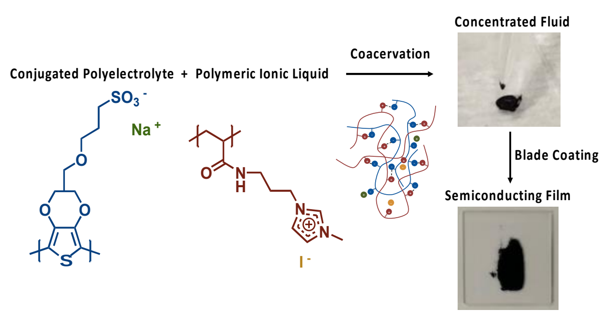

Aqueous formulation of conjugated polymers enables environmentally benign processing routes, fabrication of multi-layer devices *via* deposition from varying solvents, and bioelectronic applications.[1] Enhanced dissolution of conjugated polymers in water can be achieved by ionic functionalization of side chains that compensate for the hydrophobicity of the π-conjugated backbone. This class of materials, conjugated polyelectrolytes (CPEs),[2] offers orthogonal control of the material's optoelectronic properties and aqueous processability. Nonetheless, the limited solubility of CPEs in water often inhibits the ability to make concentrated solutions that are desirable for many applications.

Complexation with polyelectrolytes offers a promising route to improve the aqueous solubility of CPEs. Mixing two oppositely charged polyelectrolytes can result in formulations with much higher concentrations than simple solutions of polymers and solvents.[3] Intimate mixing of two polyelectrolytes is thermodynamically favorable because of the electrostatic attraction of charged groups, in contrast to the common immiscibility of uncharged polymers that results from a high Flory–Huggins interaction parameter χ. In certain conditions, mixing of two polyelectrolytes results in an associative liquid–liquid phase separation in which a polymer-depleted phase, the supernatant, is in coexistence with a polymer-dense phase (typically 20-30% *w/v* polymer) called the coacervate.[4] The fluid nature of the coacervate suggests its potential compatibility with industrial processing protocols such as blade coating and gravure printing.[5] Polyelectrolyte coacervation is important to several biological processes including the formation of membraneless organelles [6,7] and underwater adhesives, [8,9] and has been widely proposed for new biotechnologies.[10–12] Since the first observation of coacervation almost a century ago,[13,14] much effort has been devoted to elucidating a general theoretical thermodynamic framework, phase behavior, dynamics and mechanics, and self-assembled structure of polyelectrolyte complex coacervates.[15–27]

Despite this large body of literature on non-conjugated polyelectrolytes, coacervation has only been reported in a few conjugated polymer systems.[3,28] For example, the coacervation between a polythiophene-based CPE and an insulating polyelectrolyte in THF/water solvent mixtures has been shown to increase the CPE's conjugation length and photoluminescence yield.[3] CPE–polyelectrolyte coacervation was also reported to occur in aqueous high-salt media, with the mixture's phase behavior and photophysical properties showing a strong dependence on the identity of the cation salt.[28] Studies on CPE-CPE complexation in salt-free water,[29,30] focusing on dilute regimes and the solid-state complexes, have further elucidated how the inclusion of the conjugated moieties fundamentally affects complexation thermodynamics. Similar to the CPE–polyelectrolyte coacervate, complexation of two CPEs in the dilute regime was shown to induce extension and planarization of the CPE backbone. Lastly, a study on the complexation between a di-block(neutral conjugated polymer-CPE) and DNA in dilute environments points out that the microstructure of the complex and the photophysical properties of the conjugated components could be tunned via modification of the polycation-polyanion mixing ratio.[31] Together, these studies demonstrate that polyelectrolyte complexation can be utilized as a highly versatile self-assembly motif to formulate dense coacervates of CPEs with beneficial changes in optoelectronic performance.

Prior studies have only focused on conjugated polymer complexes in the solvated state, while many electronic applications require the use of the conjugated material in the form of solvent-free solid. Thus, it is crucial to investigate processing routes for obtaining solid films from the CPE coacervate and the impacts that coacervation might have on the material's solid-state properties. Understanding these formulation—processing–property relationships will not only allow us to evaluate the properties of the solid polymer blend obtained by drying the coacervate, but also assess the practicality of this self-assembly pathway for processing of high concentration conjugated polymer solutions for use in optoelectronic devices.

Herein, we show that the aqueous coacervation between a CPE and an oppositely charged polymerized ionic liquid (PIL), an analogy to polyelectrolytes but with larger and more diffusive ionic sidechains, can be used to obtain a concentrated functional fluid of 50% *w/v* polymer. This viscous fluid was blade coated and dried to form a homogeneous solid film of μm-scale thickness. Spectroscopy and conductivity measurements of the film cast from the coacervate indicate that coacervation enhanced the conjugated length in both solvated and solid states of the CPE and, as a result, increased the charge carrier mobility along the conjugated backbone. This study suggests that polymer–polymer coacervation is a viable route for formulation of a highly concentrated semiconductive fluid phase that can be casted into solid films with enhanced optoelectronic properties.

A CPE:PIL model system was designed to achieve highly tunable ionic interactions between two polymers and to facilitate the doping of the CPE component. An alkyl sulfonate derivative of poly(3,4-ethylenedioxythiophene) with sodium counter-ions (PEDOT-S, Figure 1) was chosen as the CPE. The dioxane ring has been shown to donate electron density to the thiophene ring and thus lowers the band gap and the oxidation potential of EDOT-based polymers relative to polythiophenes.[32,33] Moreover, the oxygen atoms on the dioxane ring give PEDOT-S the capability to accept hydrogen bonds, enhancing the polymer solubility in water. For the PIL, a polyacrylamide backbone with methyl-imidazolium functionalized side chains and iodine counter-ions was used (PA-MPI, Figure 1). The wide electrochemical stability window of the imidazolium group [34] allows it to remain stable upon electrical doping of the CPE coacervate. PEDOT-S and PA-MPI polymers were obtained *via* oxidative polymerization and reversible addition-fragmentation chain transfer polymerizations (Figure S1 and S2). The number-average molecular weights are 16 kDa for PEDOT-S (relative to a Bovine Serum Albumin (BSA) standard in aqueous Gel-Permeation Chromatography) and 13 kDa for PA-MPI (obtained *via* NMR end group analysis). We note that PEDOT-S has a high dispersity (Đ=1.95 relative to PSS standard) due to the nature of oxidative polymerization.

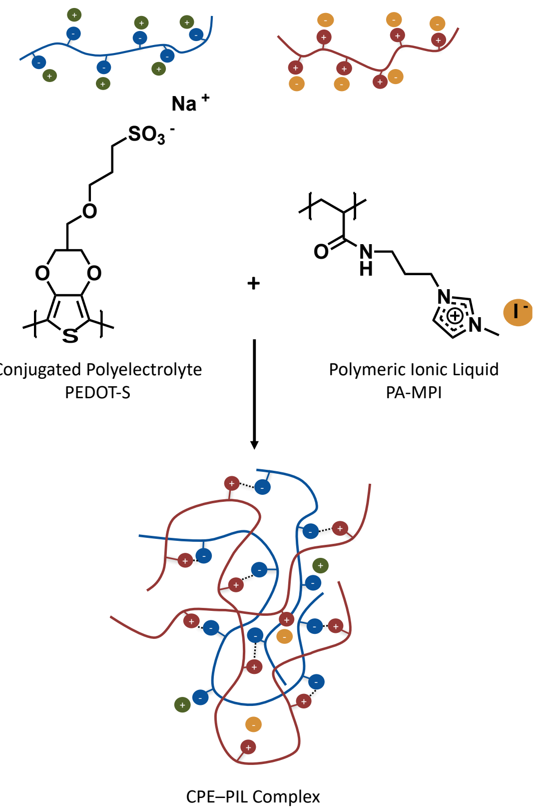

Figure 1. Chemical structures of PA-MPI (polycation) and PEDOT-S (polyanion) and their formation of a polyelectrolyte complex upon mixing.

The phase behavior of the CPE:PIL complex, which was examined by varying the concentration aqueous KBr solvent and the concentration of the polymers in the stock solutions, shows a wide coacervate window that stretches across a broad region of the phase diagram (Figure 2). In particular, the coexistence of the coacervate and the supernatant was absent only in the diagram's top-left and the bottom-right corners. In the high-salt-low-polymer region (top-left), the strong electrostatic screening from the added ionic strength suppresses the charge-mediated complexation between the CPE and the PIL. As a result, only 1-phase solutions form in these conditions. In the low-salt-high-polymer region (bottom-right), the strong electrostatic interactions trap the complex structure to form a dense complex. This phase is commonly referred to as the precipitate.[35] Due to its solid-like nature, the precipitate is much more challenging to process than the coacervate. The CPE:PIL coacervate was observed in the rest of the phase diagram, covering the majority of the mixing conditions where the balance between ionic screening and kinetics was maintained. The PEDOT-S:PA-MPI phase diagram therefore suggests the processability of the complex across a wide range of accessible compositions.

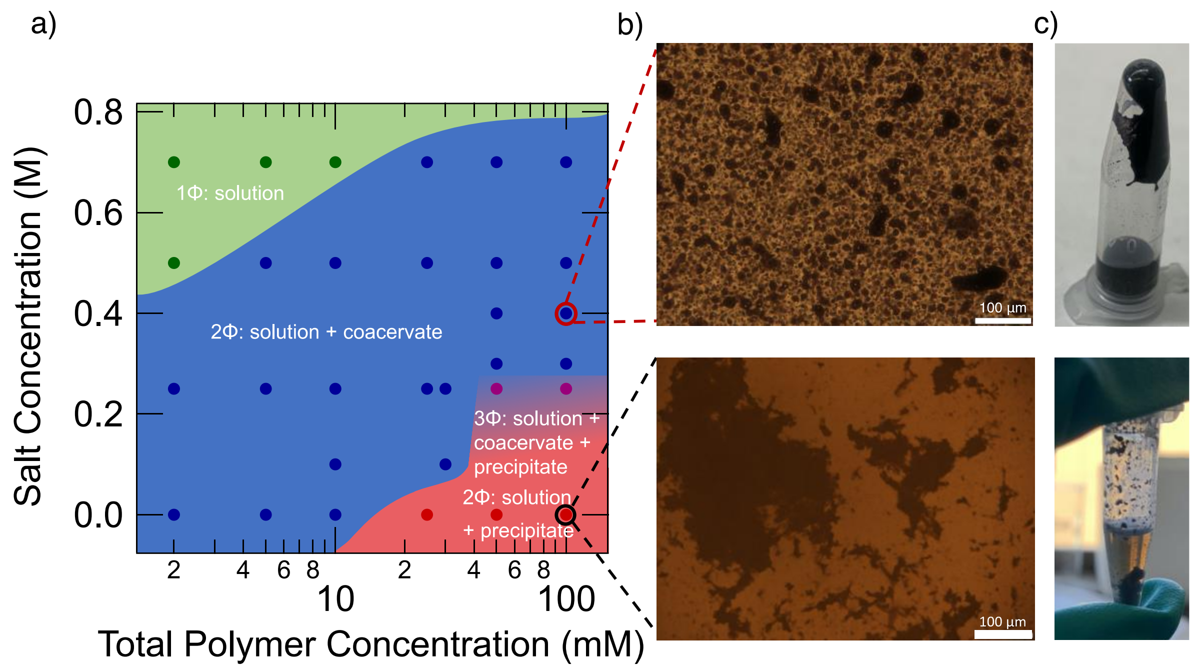

Figure 2. (a) Phase diagram of PEDOT-S and PA-MPI as a function of solvent KBr concentration and total polymer concentration. The coacervate–solution coexistence region covers the majority of the accessible phase diagram. At high polymer concentrations and intermediate ionic strength (~0.25M KBr solution), there was a crossover "three phase" region in which both the coacervate and the precipitate were in co-existence with the supernatant (b) Optical microscopy images and (c) color photographs of the coacervate (upper) and the precipitate (lower) phases in coexistence with their supernatant phases. The complexed phases are distinctive by optical microscopy and by their macroscopic behavior. Both the coacervate and precipitate are optically dense due to the high concentration of CPE while the solution is less optically dense. At the macroscopic scale, the precipitate appears as dense solid chunks aggregated at the bottom of the Eppendorf tube, while the coacervate has more liquid-like behavior and sticks to the tube walls upon centrifugation.

For the following studies of thin solid films, the coacervate was used because of its increased processability relative to the precipitate. The 100mM total polymer with 0.5M KBr condition was chosen, as it is well within the coacervate region in the phase diagram. For processing and characterization of the coacervate, the mixture was centrifuged to promote complete coalescence of the coacervate droplets. This coacervate was highly concentrated with 50% *w/v* polymer and was left in contact with the supernatant phase to preserve the equilibrium conditions until ready for use.

Interestingly, the complexation process with the PIL only induces a minimal change in the chain conformation of PEDOT-S possibly due to the stiffer nature of this polymer relative to other CPEs. As shown in Figure 3, the π–π* electronic transition peaks of the stock CPE solution and the coacervate are both at ≈ 2.2 eV, with the coacervate's absorption peak shifted slightly to lower energies. Red shifts in the absorption peak were previously reported in polymer–small molecule [36] and polymer–polymer [3,28,29] complex systems and were attributed to the reduction in conformational disorder along the conjugated backbone leading to an increase in the conjugation length. A Gaussian fitting procedure was performed on both spectra, deconvoluting this peak into two overlapping peaks (Figure S3 and S4) whose positions red-shifted minimally (~ 0.02 eV) upon coacervation. This observation is fundamentally different from our previously reported results, where much larger red-shifts (up to 0.25 eV) in the absorption peak of (poly{3-[6′-(N-butylimidazolium)-hexyl]thiophene}bromide ($P3BImHT^+:Br^-$) were observed upon the CPE's complexation with sodium poly(styrenesulfonate) ($Na^+:PSS^-$).[3] However, in a recent study, the complexation between poly(fluorene-*alt*-phenylene) (PFPI) and $Na^+:PSS^-$ was reported to lead to red-shifts of only 0.04 – 0.08 eV in the absorption profile of the CPE.[28] Thus, it is likely that the higher rigidity of PEDOT-S and PFPI backbones compared to $P3BImHT^+:Br^-$ made these polymers less susceptible to conformational changes upon complexation.

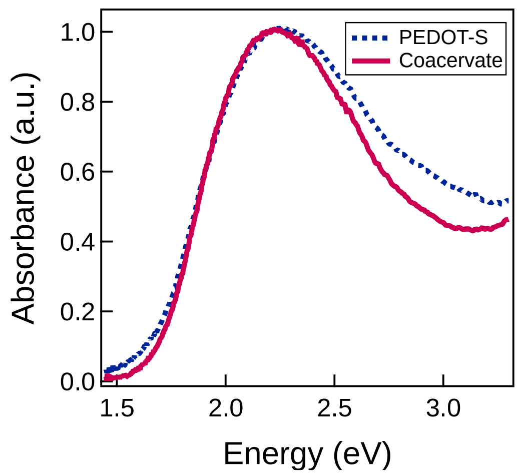

Figure 3. UV-Vis spectra of PEDOT-S in stock CPE solution form and in the swollen complex coacervate. The position of the optical absorption peak slightly red-shifted upon coacervation, suggesting a small enhancement in the conjugation length of PEDOT-S upon coacervation.

Due to its high solids loading and viscous nature, the PEDOT-S:PA-MPI coacervate can be easily blade coated to form a solid film with little thickness loss upon drying (~ 4.0 ± 0.5 μm). The preparation of the coacervate in an aqueous KBr solution led to the partition of salt ions into the cast film. Elemental analysis of the solid film cast from the coacervate confirmed the presence of K and Br (Table S1) indicating doping by the salt. Nonetheless, these ions can be removed easily from the coacervate by immersing the resulting film in milli-Q water overnight to promote diffusion of salt ions out of the film.

The lyophilic nature of the coacervate stabilizes the hydrophobic CPE backbone in a gel-like homogeneous network instead of forming collapsed aggregates with hydrophilic outer shell (for example as PEDOT:PSS). The homogeneous distribution of the conjugated material in the coacervate is indicated by the homogeneous intensity of brown of the coacervate droplets in the microscopic image (Figure 2). Memory of the conformations from the solvated-coacervate appears to be retained in the solid-state, as indicated by the homogeneous morphology of the complex film (scanning electron microscope (SEM) images of the film, Figure 4).

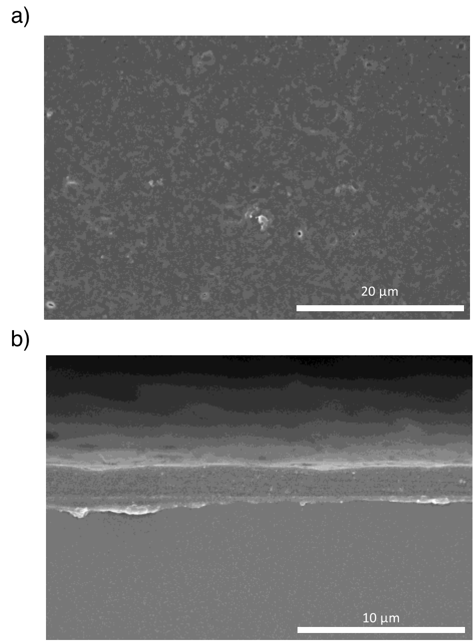

Figure 4. (a) Top view and (b) side view SEM images of a dry film cast from the coacervate after salt removal.

Electronic charge carriers could be introduced into the solid formed from the coacervate via doping to form electrically conductive films. In this study, we introduced the dopant from the vapor phase to not disturb the coacervate assembly. Other methods such as doping in solution,[37–39] solution-sequential doping,[40] and immersion doping,[41] which have been successfully utilized with neat semiconducting polymers, introduced complications in processing. In particular, when doping in solution was attempted, the additional charges along the doped CPE backbone led to preferential formation of the dense precipitate over the weakly complexed coacervate. The use of salt to effectively screen the strong electrostatic interactions within the doped system was counteracted by the poor solubility of doped PEDOT-S in aqueous solution with large levels of added salt. Immersion doping and solution-sequential doping did not interrupt the mixing phase behavior but disrupted the structure of the solid film cast from the coacervate. We attribute this observation to the ionic cross-linking within the polymer–polymer complex breaking up by infiltration of dopant molecules into the film in the presence of a solvent, analogous to the partitioning of salt. As a result, the complex film partially dissolved or detached from the substrate. The infiltration of a dopant from the vapor phase, in contrast, not only ensured the formation of the coacervate phase (prior to doping) but also minimized interruption to the complexed structure during doping. HTFSI was chosen to be the dopant, as this strong acid vapor has been used effectively in doping of other conjugated polymers [42] and the resulting TFSI anion has good thermal and chemical stability. Moreover, the low sublimation temperature of HTFSI allows the doping process to be carried out at relatively low temperature, which is desirable for preserving the coacervate film structure.[43]

Effective electronic doping of the complex film was evidenced by the emergence of the polaronic features (1.2 – 1.5 eV) and the bleaching of the neutral polymer peak at 2.2 eV in the optical absorption spectrum of the film upon doping (Figure 5). Interestingly, we also observe a shift to lower energy when comparing the polaronic absorption peaks of the doped coacervate and doped CPE films. This agreement between the optical spectra of doped and pristine samples confirms the enhancement in the conjugation length of the CPE upon coacervation that leads to more delocalized polaron along the CPE backbone.

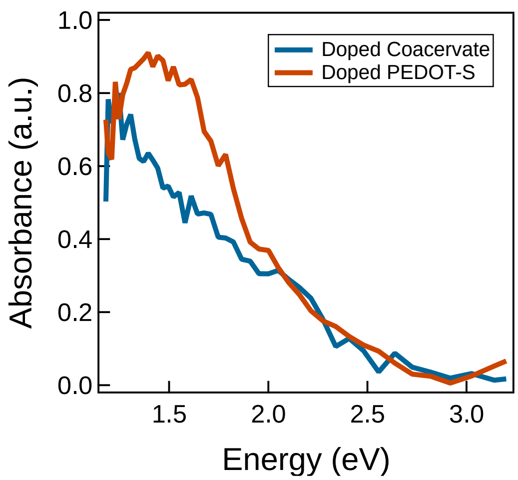

Figure 5. UV-Vis spectra of PEDOT-S and complex films doped with HTFSI vapor. The position of the polaron peak was red-shifted upon coacervation, indicating more delocalization of the radical cation along complexed PEDOT-S backbone.

Consistent with the conjugation length enhancement of the CPE observed in the UV-Vis spectra, coacervation appears to have increased the charge carrier mobility of PEDOT-S. In particular, the conductivity of the complex film at the optimal doping level was 2 $\times 10^{-4}$ S cm^{-1}, twice that of the PEDOT-S film doped by the same method. Since approximately half of the material in the coacervate was insulating, this difference in conductivity suggests a higher charge-carrier mobility in the coacervate than in the PEDOT-S film.

Beyond enhancing the conjugation of the CPE, coacervation may have possibly increased the conductivity of the coacervate by the partitioning of longer chains in the coacervate relative to the stock CPE sample from which it was formed. Higher fractions of long polymer chains have been shown to increase charge carrier mobility due to the enhancement in intrachain charge transport.[44] There are two possible driving forces for this partitioning of long chains into the coacervate. Firstly, longer chains have smaller reduction of translational entropy upon coacervation. Secondly, longer polymer chains likely have poor solubility in the supernatant phase, as elemental analysis of the film casted from the coacervate indicates the preferential partitioning of KBr into the supernatant and thus making it a high-salt environment (Table S1.) Previous studies on conventional polyelectrolyte coacervate also reported the preferential partitioning of long polymer chains from stock solution into the coacervate phase, as indicated by a higher average radius of gyration (R_g) of the polymer in the coacervate than that in the stock polymer solution.[45] We note that the high polydispersity of our PEDOT-S sample might further amplify the impact of long-chain-partitioning.

It appears that the enhanced charge carrier mobility is unlikely to be a caused by changes in ordering, as both the neat PEDOT-S and the coacervate are amorphous with no evidence of long-range ordering in X-ray scattering (Figure S5). This lack of crystallinity in both PEDOT-S and the complex films also explains their relatively low conductivities compared to some other conjugated polymers. It is likely that the highly charged nature (charge fraction f = 1) and the uncontrolled regiochemistry of PEDOT-S synthesis have prevented sufficient interchain packing in these materials.

Interestingly, we also observed excellent ion solvation by the CPE:PIL complex film. At the optimal electronic doping level, a room-temperature ionic conductivity of 9×10^{-5} S cm^{-1} was measured. Since the complete removal of KBr was confirmed *via* XPS, this ionic conductivity was contributed solely by HTFSI. XPS elemental analysis of the film supports this observation: the F/S ratio, which is an indication of the amount of TFSI anion relative to PEDOT-S, in the doped complex film was approximately 2 times higher than in the doped PEDOT-S film (Table S1). Etching experiments performed on the complex film show this trend to be consistent through the film's μm-scale depth. These results indicate that upon its infiltration to the complex film, HTFSI not only doped the PEDOT-S backbone but also act as an ionic dopant, possibly by partitioning into the side chain regions (Figure 6). A major driving force for this process is likely the much lower pKa of HTFSI (pKa ~ -12) [46] compared to that of polymerized sulfonic acid, whose pKa decreases with higher degree of polymerization and plateaus at around 2.9 for poly(styrene sulfonic acid).[47] This significant difference in pKa makes the association of protons with PEDOT-S side chains preferential over TFSI anions. It is not clear whether HTFSI partitions first into the side chain regions or dopes the PEDOT-S backbone. Nonetheless, the relatively high ionic conductivity of the complex at room temperature indicates that this CPE:PIL complex can solvate and facilitate the transport of a significant number of ions in solvent-free conditions, suggesting its great potential as a solid-state ion conductor.

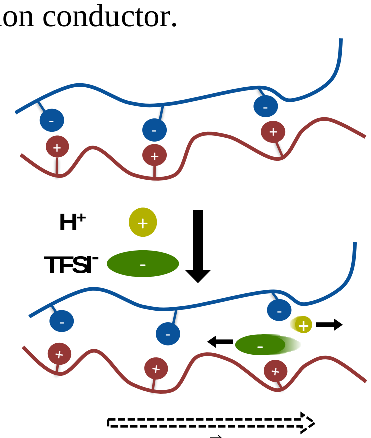

Figure 6. Schematic of the partitioning of HTFSI into the coacervate system and the contribution of the dissociated protons and TFSI anions to the observed ionic conductivity.

We have shown that CPE:PIL coacervation provides a promising route for processing of conjugated polymers in aqueous media at exceptionally higher polymer concentrations (50% *w/v* polymer) than conventional solution processing methods (~ 1% *w/v* polymer). The resulting coacervate fluid is compatible with large-scale processing methods such as blade coating, and the highly concentrated nature of this material enables the fabrication of µm-thick films. Thick films also possess advantages over thin (100s nm) films in some applications such as thermoelectrics [48] and pressure sensors.[49] This approach is highly versatile for use in CPE systems, as the complexation process can be easily tuned by changing mixing conditions such as solvent dielectric strength and polymer concentration. Salt is often needed to achieve the fluidic coacervate phase, yet the salt ions remaining in the coacervate can be removed easily at the end of the film casting process.

Beyond advantages in processing, coacervation also can positively impact the optoelectronic performance of conjugated polymers. In particular, a reduction in conformational disorder along the CPE backbone upon its coacervation with another polyelectrolyte results in enhanced conjugation length and higher charge carrier mobility. Thus, the process of polyelectrolyte coacervation could also be utilized for improved performance of organic optoelectronic devices.

While not investigated in this study, it is expected that tuning of other factors such as the Flory–Huggins parameter and the mixing ratio of the two polyelectrolytes could result in interesting morphological changes of the coacervate from a homogeneous, disordered complex to microphase-separated structure,[50,51] or even macrophases rich in either the polycation or polyanion.[52–54] These changes in morphology will likely affect the electronic conduction pathway and as a result the transport property of the coacervate drastically. An analogous trend has been observed with PEDOT:PSS, where a significant improvement in the electrical conductivity of this material was achieved by promoting microphase-segregation within the complex to produce PEDOT-rich and PSS-rich domains.[55] Thus, further studies toward the manipulation of the complexation process to access different morphologies are needed to provide a more thorough understanding of the structure—properties relationships in this system.

ASSOCIATED CONTENT

Supporting Information.

Synthetic and characterization procedures, XPS elemental analysis, UV-Vis spectroscopy peak fit, X-ray structural characterization, and Electrochemical Impedance Spectroscopy measurement.

AUTHOR INFORMATION

Corresponding Authors

Email: mchabinyc@engineering.ucsb.edu

Email: segalman@ucsb.edu

ORCID

My Linh Le: 0000-0003-2385-0385
Dakota Rawlings: 0000-0003-4025-8017
Rhys M. Kennard: 0000-0003-1181-5638
Michael L. Chabinyc: 0000-0003-4641-3508
Scott P. O. Danielsen: 0000-0003-3432-5578
Rachel A. Segalman: 0000-0002-4292-5103

Notes

The authors declare no competing financial interest

ACKNOWLEDGEMENTS

The authors acknowledge funding support from the Department of Energy Office of Basic Energy Sciences under grant no. DE-SC0016390. The authors acknowledge the use of shared facilities of the UCSB MRSEC (NSF DMR 1720256), a member of the Materials Research Facilities Network (www.mrfn.org) and the use of the Nanostructures Cleanroom Facility within the California NanoSystems Institute, supported by the University of California, Santa Barbara and the University of California, Office of the President. This research used resources of the National Synchrotron Light Source II, a U.S. Department of Energy Office of Science User Facility (DE-SC0012704; beamline 11-BM). The authors thank Dr. Thomas Mates for XPS and Dr. Rachel Behrens for GPC data acquisition and analysis.

References

(1) Savagian, L. R.; Österholm, A. M.; Ponder, J. F.; Barth, K. J.; Rivnay, J.; Reynolds, J. R. Balancing Charge Storage and Mobility in an Oligo(Ether) Functionalized Dioxythiophene Copolymer for Organic- and Aqueous- Based Electrochemical Devices and Transistors. *Adv. Mater.* **2018**, *30* (50), 1804647. https://doi.org/10.1002/adma.201804647.

(2) Pinto, M. R.; Scinanze, K. S. Conjugated Polyelectrolytes: Synthesis and Applications. **2002**.

(3) Danielsen, S. P. O.; Nguyen, T. Q.; Fredrickson, G. H.; Segalman, R. A. Complexation of a Conjugated Polyelectrolyte and Impact on Optoelectronic Properties. *ACS Macro Lett.* **2019**, *8* (1), 88–94. https://doi.org/10.1021/acsmacrolett.8b00924.

(4) G Bungenberg De Jong, B. H.; Kruyt, H. R. *Chemistry.-Coacervation (Partial Miscibility in Colloid Systems). (Preliminary Communication)*; 1929.

(5) Søndergaard, R. R.; Hösel, M.; Krebs, F. C. Roll-to-Roll Fabrication of Large Area

Functional Organic Materials. *Journal of Polymer Science, Part B: Polymer Physics*. Wiley Periodicals, Inc January 1, 2013, pp 16–34. https://doi.org/10.1002/polb.23192.
(6) Hyman, A. A.; Weber, C. A.; Ulicher, F. J. ¨. Liquid-Liquid Phase Separation in Biology. *Annu. Rev. Cell Dev. Biol* **2014**, *30*, 39–58. https://doi.org/10.1146/annurev-cellbio-100913-013325.
(7) Banani, S. F.; Lee, H. O.; Hyman, A. A.; Rosen, M. K. Biomolecular Condensates: Organizers of Cellular Biochemistry. *Nature Reviews Molecular Cell Biology*. Nature Publishing Group May 1, 2017, pp 285–298. https://doi.org/10.1038/nrm.2017.7.
(8) Wei, W.; Tan, Y.; Martinez Rodriguez, N. R.; Yu, J.; Israelachvili, J. N.; Waite, J. H. A Mussel-Derived One Component Adhesive Coacervate. *Acta Biomater.* **2014**, *10* (4), 1663–1670. https://doi.org/10.1016/j.actbio.2013.09.007.
(9) Hwang, D. S.; Zeng, H.; Srivastava, A.; Krogstad, D. V.; Tirrell, M.; Israelachvili, J. N.; Waite, J. H. Viscosity and Interfacial Properties in a Mussel-Inspired Adhesive Coacervate. *Soft Matter* **2010**, *6* (14), 3232–3236. https://doi.org/10.1039/c002632h.
(10) Sing, C. E.; Perry, S. L. Recent Progress in the Science of Complex Coacervation. *Soft Matter* **2020**, *16* (12), 2885–2914. https://doi.org/10.1039/d0sm00001a.
(11) Macleod, G. S.; Collett, J. H.; Fell, J. T. The Potential Use of Mixed Films of Pectin, Chitosan and HPMC for Bimodal Drug Release. *J. Control. Release* **1999**, *58* (3), 303–310. https://doi.org/10.1016/S0168-3659(98)00168-0.
(12) Genta, I.; Perugini, P.; Modena, T.; Pavanetto, F.; Castelli, F.; Muzzarelli, R. A. A.; Muzzarelli, C.; Conti, B. Miconazole-Loaded 6-Oxychitin-Chitosan Microcapsules. *Carbohydr. Polym.* **2003**, *52* (1), 11–18. https://doi.org/10.1016/S0144-8617(02)00257-6.
(13) G Bungenberg De Jong, B. H.; Kruyt, H. R. *Chemistry.-Coacewation (Partial Miscibility in Colloid Systems). (Preliminary Communication)*; 1929.
(14) Overbeek, J. T. G.; Voorn, M. J. Phase Separation in Polyelectrolyte Solutions. Theory of Complex Coacervation. *J. Cell. Comp. Physiol.* **1957**, *49* (S1), 7–26. https://doi.org/10.1002/jcp.1030490404.
(15) Manoj Lalwani, S.; Eneh, C. I.; Lutkenhaus, J. L. Emerging Trends in the Dynamics of Polyelectrolyte Complexes. *Physical Chemistry Chemical Physics*. Royal Society of Chemistry November 14, 2020, pp 24157–24177. https://doi.org/10.1039/d0cp03696j.
(16) Lytle, T. K.; Sing, C. E. Tuning Chain Interaction Entropy in Complex Coacervation Using Polymer Stiffness, Architecture, and Salt Valency. *Mol. Syst. Des. Eng.* **2018**, *3* (1), 183–196. https://doi.org/10.1039/c7me00108h.
(17) Danielsen, S. P. O.; Panyukov, S.; Rubinstein, M. Ion Pairing and the Structure of Gel Coacervates. *Macromolecules* **2020**, *53* (21), 9420–9442. https://doi.org/10.1021/acs.macromol.0c01360.
(18) Rubinstein, M.; Liao, Q.; Panyukov, S. Structure of Liquid Coacervates Formed by Oppositely Charged Polyelectrolytes. *Macromolecules* **2018**, *51* (23), 9572–9588. https://doi.org/10.1021/acs.macromol.8b02059.
(19) Delaney, K. T.; Fredrickson, G. H. Theory of Polyelectrolyte Complexation - Complex Coacervates Are Self-Coacervates. *J. Chem. Phys.* **2017**, *146* (22), 224902. https://doi.org/10.1063/1.4985568.
(20) Danielsen, S. P. O.; McCarty, J.; Shea, J. E.; Delaney, K. T.; Fredrickson, G. H. Small Ion Effects on Self-Coacervation Phenomena in Block Polyampholytes. *J. Chem. Phys.* **2019**, *151* (3), 34904. https://doi.org/10.1063/1.5109045.
(21) Yang, M.; Shi, J.; Schlenoff, J. B. Control of Dynamics in Polyelectrolyte Complexes by

Temperature and Salt. *Macromolecules* **2019**, *52* (5), 1930–1941. https://doi.org/10.1021/acs.macromol.8b02577.
(22) Fares, H. M.; Ghoussoub, Y. E.; Delgado, J. D.; Fu, J.; Urban, V. S.; Schlenoff, J. B. Scattering Neutrons along the Polyelectrolyte Complex/Coacervate Continuum. *Macromolecules* **2018**, *51* (13), 4945–4955. https://doi.org/10.1021/acs.macromol.8b00699.
(23) Blocher McTigue, W. C.; Perry, S. L. Protein Encapsulation Using Complex Coacervates: What Nature Has to Teach Us. *Small*. Wiley-VCH Verlag July 1, 2020, p 1907671. https://doi.org/10.1002/smll.201907671.
(24) Friedowitz, S.; Salehi, A.; Larson, R. G.; Qin, J. Role of Electrostatic Correlations in Polyelectrolyte Charge Association. *J. Chem. Phys.* **2018**, *149* (16), 163335. https://doi.org/10.1063/1.5034454.
(25) Salehi, A.; Larson, R. G. A Molecular Thermodynamic Model of Complexation in Mixtures of Oppositely Charged Polyelectrolytes with Explicit Account of Charge Association/Dissociation. *Macromolecules* **2016**, *49* (24), 9706–9719. https://doi.org/10.1021/acs.macromol.6b01464.
(26) Hamad, F. G.; Chen, Q.; Colby, R. H. Linear Viscoelasticity and Swelling of Polyelectrolyte Complex Coacervates. *Macromolecules* **2018**, *51* (15), 5547–5555. https://doi.org/10.1021/acs.macromol.8b00401.
(27) Larson, R. G.; Liu, Y.; Li, H. Linear Viscoelasticity and Time-Temperature-Salt and Other Superpositions in Polyelectrolyte Coacervates. *J. Rheol. (N. Y. N. Y).* **2021**, *65* (1), 77–102. https://doi.org/10.1122/8.0000156.
(28) Johnston, A. R.; Perry, S. L.; Ayzner, A. L. Associative Phase Separation of Aqueous π-Conjugated Polyelectrolytes Couples Photophysical and Mechanical Properties. **2021**. https://doi.org/10.1021/acs.chemmater.0c02424.
(29) Hollingsworth, W. R.; Segura, C.; Balderrama, J.; Lopez, N.; Schleissner, P.; Ayzner, A. L. Exciton Transfer and Emergent Excitonic States in Oppositely-Charged Conjugated Polyelectrolyte Complexes. *J. Phys. Chem. B* **2016**, *120* (31), 7767–7774. https://doi.org/10.1021/acs.jpcb.6b06533.
(30) Hollingsworth, W. R.; Williams, V.; Ayzner, A. L. Semiconducting Eggs and Ladders: Understanding Exciton Landscape Formation in Aqueous π-Conjugated Inter-Polyelectrolyte Complexes. **2020**. https://doi.org/10.1021/acs.macromol.0c00029.
(31) Knaapila, M.; Costa, T.; Garamus, V. M.; Kraft, M.; Drechsler, M.; Scherf, U.; Burrows, H. D. Polyelectrolyte Complexes of a Cationic All Conjugated Fluorene-Thiophene Diblock Copolymer with Aqueous DNA. *J. Phys. Chem. B* **2015**, *119* (7), 3231–3241. https://doi.org/10.1021/jp5110032.
(32) Ponder, J. F.; Österholm, A. M.; Reynolds, J. R. Designing a Soluble PEDOT Analogue without Surfactants or Dispersants. *Macromolecules* **2016**, *49* (6), 2106–2111. https://doi.org/10.1021/acs.macromol.5b02638.
(33) Reeves, B. D.; Grenier, C. R. G.; Argun, A. A.; Cirpan, A.; McCarley, T. D.; Reynolds, J. R. Spray Coatable Electrochromic Dioxythiophene Polymers with High Coloration Efficiencies. *Macromolecules* **2004**, *37* (20), 7559–7569. https://doi.org/10.1021/ma049222y.
(34) Kazemiabnavi, S.; Zhang, Z.; Thornton, K.; Banerjee, S. Electrochemical Stability Window of Imidazolium-Based Ionic Liquids as Electrolytes for Lithium Batteries. *J. Phys. Chem. B* **2016**, *120* (25), 5691–5702. https://doi.org/10.1021/acs.jpcb.6b03433.

(35) Kulkarni, A. D.; Vanjari, Y. H.; Sancheti, K. H.; Patel, H. M.; Belgamwar, V. S.; Surana, S. J.; Pardeshi, C. V. Polyelectrolyte Complexes: Mechanisms, Critical Experimental Aspects, and Applications. *Artif. Cells, Nanomedicine, Biotechnol.* **2016**, *44* (7), 1615–1625. https://doi.org/10.3109/21691401.2015.1129624.

(36) Evans, R. C.; Knaapila, M.; Willis-Fox, N.; Kraft, M.; Terry, A.; Burrows, H. D.; Scherf, U. Cationic Polythiophene-Surfactant Self-Assembly Complexes: Phase Transitions, Optical Response, and Sensing. *Langmuir* **2012**, *28* (33), 12348–12356. https://doi.org/10.1021/la302166a.

(37) Pingel, P.; Neher, D. Comprehensive Picture of P-Type Doping of P3HT with the Molecular Acceptor F4TCNQ. *Phys. Rev. B - Condens. Matter Mater. Phys.* **2013**, *87* (11), 115209. https://doi.org/10.1103/PhysRevB.87.115209.

(38) Duong, D. T.; Wang, C.; Antono, E.; Toney, M. F.; Salleo, A. The Chemical and Structural Origin of Efficient P-Type Doping in P3HT. *Org. Electron.* **2013**, *14* (5), 1330–1336. https://doi.org/10.1016/j.orgel.2013.02.028.

(39) Wang, C.; Duong, D. T.; Vandewal, K.; Rivnay, J.; Salleo, A. Optical Measurement of Doping Efficiency in Poly(3-Hexylthiophene) Solutions and Thin Films. *Phys. Rev. B - Condens. Matter Mater. Phys.* **2015**, *91* (8), 085205. https://doi.org/10.1103/PhysRevB.91.085205.

(40) Scholes, D. T.; Hawks, S. A.; Yee, P. Y.; Wu, H.; Lindemuth, J. R.; Tolbert, S. H.; Schwartz, B. J. Overcoming Film Quality Issues for Conjugated Polymers Doped with F4TCNQ by Solution Sequential Processing: Hall Effect, Structural, and Optical Measurements. *J. Phys. Chem. Lett.* **2015**, *6* (23), 4786–4793. https://doi.org/10.1021/acs.jpclett.5b02332.

(41) Kolesov, V. A.; Fuentes-Hernandez, C.; Chou, W. F.; Aizawa, N.; Larrain, F. A.; Wang, M.; Perrotta, A.; Choi, S.; Graham, S.; Bazan, G. C.; Nguyen, T. Q.; Marder, S. R.; Kippelen, B. Solution-Based Electrical Doping of Semiconducting Polymer Films over a Limited Depth. *Nat. Mater.* **2017**, *16* (4), 474–481. https://doi.org/10.1038/NMAT4818.

(42) Hofmann, A. I.; Kroon, R.; Yu, L.; Müller, C. Highly Stable Doping of a Polar Polythiophene through Co-Processing with Sulfonic Acids and Bistriflimide. *J. Mater. Chem. C* **2018**, *6* (26), 6905–6910. https://doi.org/10.1039/C8TC01593G.

(43) Evans, C. M.; Bridges, C. R.; Sanoja, G. E.; Bartels, J.; Segalman, R. A. Role of Tethered Ion Placement on Polymerized Ionic Liquid Structure and Conductivity: Pendant versus Backbone Charge Placement. *ACS Macro Lett.* **2016**, *5* (8), 925–930. https://doi.org/10.1021/acsmacrolett.6b00534.

(44) Gu, K.; Snyder, C. R.; Onorato, J.; Luscombe, C. K.; Bosse, A. W.; Loo, Y. L. Assessing the Huang-Brown Description of Tie Chains for Charge Transport in Conjugated Polymers. *ACS Macro Lett.* **2018**, *7* (11), 1333–1338. https://doi.org/10.1021/acsmacrolett.8b00626.

(45) Spruijt, E.; M Leermakers, F. A.; Fokkink, R.; Schweins, R.; van Well, A. A.; Cohen Stuart, M. A.; van der Gucht, J. Structure and Dynamics of Polyelectrolyte Complex Coacervates Studied by Scattering of Neutrons, X-Rays, and Light. **2013**. https://doi.org/10.1021/ma400132s.

(46) Patel, S. N.; Glaudell, A. M.; Peterson, K. A.; Thomas, E. M.; O'Hara, K. A.; Lim, E.; Chabinyc, M. L. Morphology Controls the Thermoelectric Power Factor of a Doped Semiconducting Polymer. *Sci. Adv.* **2017**, *3* (6), e1700434. https://doi.org/10.1126/sciadv.1700434.

(47) Dong, H.; Du, H.; Wickramasinghe, S. R.; Qian, X. The Effects of Chemical Substitution and Polymerization on the PK a Values of Sulfonic Acids. *J. Phys. Chem. B* **2009**, *113* (43), 14094–14101. https://doi.org/10.1021/jp906087c.
(48) Russ, B.; Glaudell, A.; Urban, J. J.; Chabinyc, M. L.; Segalman, R. A. Organic Thermoelectric Materials for Energy Harvesting and Temperature Control. *Nature Reviews Materials*. Nature Publishing Group August 2, 2016, p 16050. https://doi.org/10.1038/natrevmats.2016.50.
(49) Harsányi, G.; Hahn, E. Thick-Film Pressure Sensors. *Mechatronics* **1993**, *3* (2), 167–171.
(50) Rumyantsev, A. M.; Kramarenko, E. Y.; Borisov, O. V. Microphase Separation in Complex Coacervate Due to Incompatibility between Polyanion and Polycation. **2018**. https://doi.org/10.1021/acs.macromol.8b00721.
(51) Rumyantsev, A. M.; Kramarenko, E. Y. Two Regions of Microphase Separation in Ion-Containing Polymer Solutions. *Soft Matter* **2017**, *13* (38), 6831–6844. https://doi.org/10.1039/c7sm01340j.
(52) Zhang, P.; Alsaifi, N. M.; Wu, J.; Wang, Z. G. Polyelectrolyte Complex Coacervation: Effects of Concentration Asymmetry. *J. Chem. Phys.* **2018**, *149* (16), 163303. https://doi.org/10.1063/1.5028524.
(53) Oskolkov, N. N.; Potemkin, I. I. Complexation in Asymmetric Solutions of Oppositely Charged Polyelectrolytes: Phase Diagram. *Macromolecules* **2007**, *40* (23), 8423–8429. https://doi.org/10.1021/ma0709304.
(54) Zhang, R.; Shklovskii, B. I. Phase Diagram of Solution of Oppositely Charged Polyelectrolytes. *Phys. A Stat. Mech. its Appl.* **2005**, *352* (1), 216–238. https://doi.org/10.1016/j.physa.2004.12.037.
(55) Shi, H.; Liu, C.; Jiang, Q.; Xu, J. Effective Approaches to Improve the Electrical Conductivity of PEDOT:PSS: A Review. *Adv. Electron. Mater.* **2015**, *1* (4), 1500017. https://doi.org/10.1002/aelm.201500017.